The EMBO Journal vol.6 no.8 pp.2415–2424, 1987

# An ordered pathway of snRNP binding during mammalian pre-mRNA splicing complex assembly

**Albrecht Bindereif and Michael R.Green**

Department of Biochemistry and Molecular Biology, Harvard University, 7 Divinity Avenue, Cambridge MA 02138, USA

Communicated by W.Keller

**We have studied the assembly, composition and structure of splicing complexes using biotin–avidin affinity chromatography and RNase protection assays. We find that U1, U2, U4, U5 and U6 snRNPs associate with the pre-mRNA and are in the mature, functional complex. Association of U1 snRNP with the pre-mRNA is rapid and ATP independent; binding of all other snRNPs occurs subsequently and is ATP dependent. Efficient binding of U1 and U2 snRNPs requires a 5′ splice site or a 3′ splice site/branch point region, respectively. Both sequence elements are required for efficient U4, U5 and U6 snRNP binding. Mutant RNA substrates containing only a 5′ splice site or a 3′ splice site/branch point region are assembled into 'partial' splicing complexes, which contain a subset of these five snRNPs. RNase protection experiments indicate that in contrast to U1 and U2 snRNPs, U4, U5 and U6 snRNPs do not contact the pre-mRNA. Based upon the time course of snRNP binding and the composition of sucrose gradient fractionated splicing complexes we suggest an assembly pathway proceeding from a 20S (U1 snRNP only) through a 40S (U1 and U2 snRNPs) to the functional 60S splicing complex (U1, U2, U4, U5 and U6 snRNPs).**

*Key words:* intron splicing/snRNPs/complex formation assembly pathway

## Introduction

During pre-mRNA splicing, the RNA substrate is rapidly assembled into a functional ribonucleoprotein (splicing) complex (reviewed in Padgett *et al.*, 1986; Green, 1986). These splicing complexes (also termed 'spliceosomes') have been detected and characterized by several methods including sucrose gradient centrifugation (Brody and Abelson, 1985; Frendewey and Keller, 1985; Grabowski *et al.*, 1985; Perkins *et al.*, 1986; Kaltwasser *et al.*, 1986; Bindereif and Green, 1986), electrophoretic separation on non-denaturing, low ionic strength gels (Pikielny and Rosbash 1986; Pikielny *et al.*, 1986; Konarska and Sharp, 1986), and RNase footprinting (Black *et al.*, 1985; Ruskin and Green, 1985a; Chabot *et al.*, 1985; Rymond and Rosbach, 1986). These studies demonstrate that splicing complex assembly precedes the first covalent modifications of the pre-mRNA, suggesting that complex formation is a prerequisite for splicing.

A major constituent of splicing complexes are small nuclear ribonucleoprotein complexes (snRNPs). Various experimental approaches have indicated that U1, U2, U4 and U6 snRNPs are splicing factors (Padgett *et al.*, 1983; Kramer *et al.*, 1984; Black *et al.*, 1985; Krainer and Maniatis, 1985; Black and Steitz, 1986; Berget and Robberson, 1986). RNase protection experiments have shown that U1 snRNP interacts with the 5′ splice site (Mount *et al.*, 1983; Black *et al.*, 1985), and U2 snRNP with the branch point (Black *et al.*, 1985; see below), and have suggested that U5 snRNP interacts directly or indirectly with the 3′ splice site (Chabot *et al.*, 1985). Whether U4 and U6 snRNPs contact any portion of or bind specific sequences within the pre-mRNA remains unknown. In addition, non-snRNP factors are required for splicing (Furneaux *et al.*, 1985; Krainer and Maniatis, 1985). Some of these, such as hnRNP C protein, have been detected in splicing complexes (Choi *et al.*, 1986).

Although U1 snRNP binds 5′ splice sites and is required for splicing, several recent studies have surprisingly reported that the U1 snRNP is not present in large splicing complexes (Konarska and Sharp, 1986; Grabowski and Sharp, 1986). These investigators have therefore suggested that U1 snRNP associates transiently with the pre-mRNA early during splicing complex assembly.

To investigate the role of U1 snRNP in splicing complex

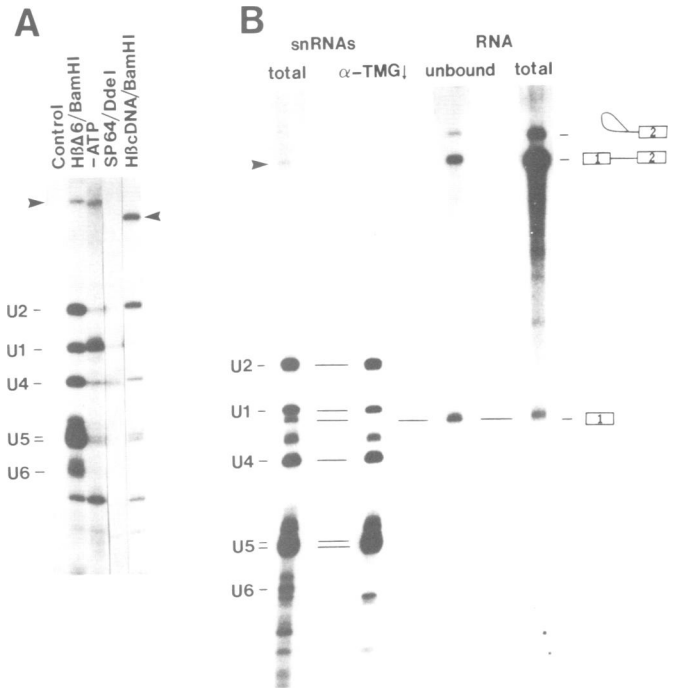


**Fig. 1.** Identification of snRNPs in splicing complexes by biotin-avidin affinity chromatography. (**A**) Splicing complexes were affinity-purified on streptavidin agarose and analyzed for bound snRNPs. U1, U2, U4, U5 and U6 snRNAs and the pre-mRNA (arrows) are indicated. SnRNA analyses are shown for the following biotinylated RNAs: SP64-HβΔ6 pre-mRNA under splicing conditions (HβΔ6/*Bam*HI) and in the absence of ATP (−ATP), SP64 RNA and HβcDNA RNA. As a control, non-biotinylated SP64-HβΔ6 RNA was analyzed for snRNP binding (control). (**B**) snRNAs isolated from affinity-purified splicing complexes (snRNAs, total) were immunoprecipitated with an anti-trimethylguanosine cap antibody (snRNAs α-TMG). U1, U2, U4, U5 and U6 snRNAs and the pre-mRNA (arrows) are indicated on the left. In addition, the distribution of pre-mRNA and splicing intermediates (schematically outlined on the right) is shown for the total splicing reaction (RNA, total) and for RNAs released from streptavidin agarose during the affinity purification (RNA, unbound).

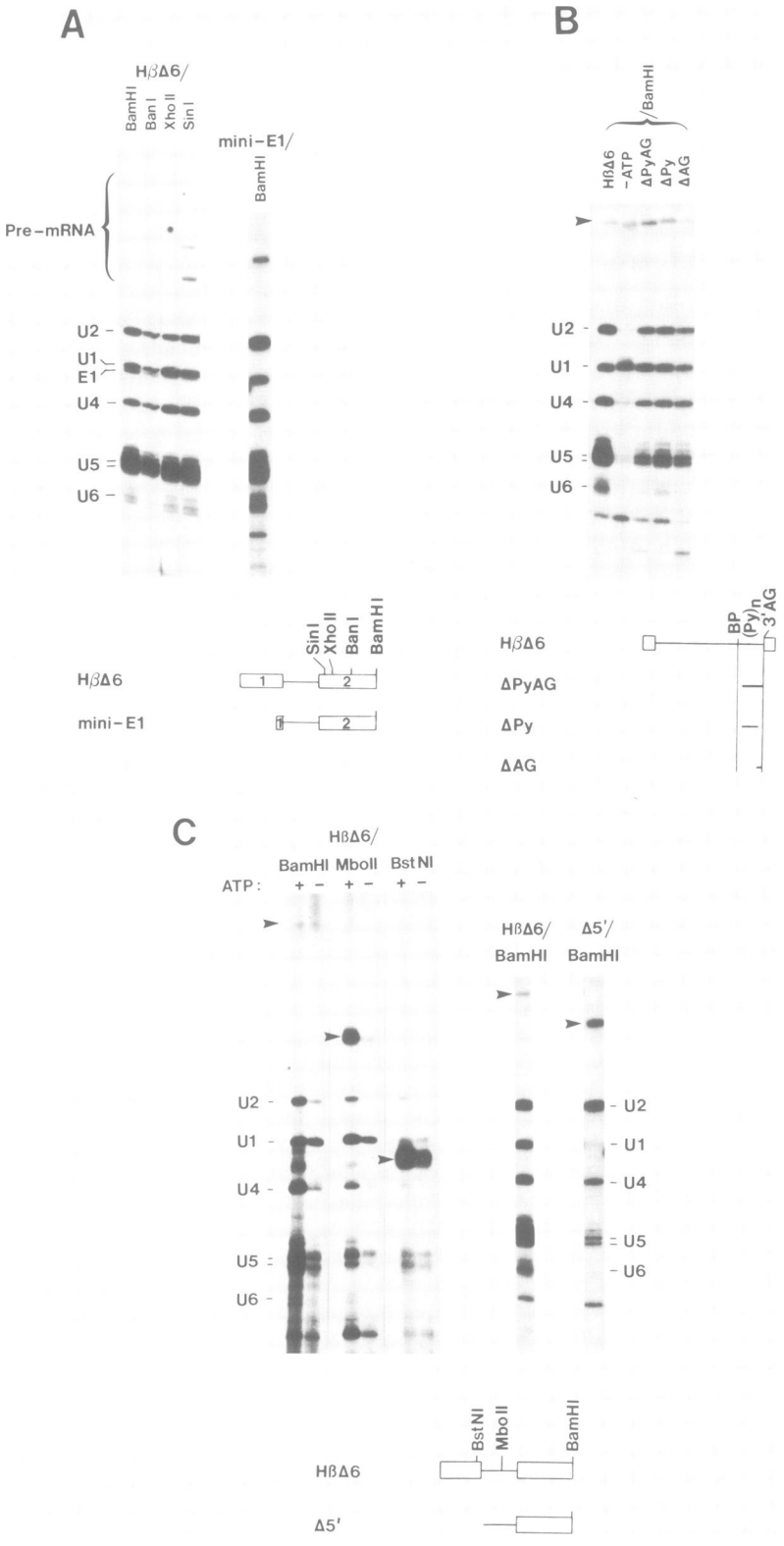


**Fig. 2.** Sequence requirements for snRNP binding. The structures of the RNAs are diagrammed below the panels. U1, U2, U4, U5 and U6 snRNAs and exon 1 as well as the pre-mRNAs (arrow) are indicated on the left for each panel. (**A**) Effect of exon truncation on snRNP binding. SP64-HβΔ6 RNAs truncated to various extents in the second exon (HβΔ6/*Bam*HI, /*Ban*I, /*Xho*II, or /*Sin*I) or containing a truncated first exon (mini-E1/*Bam*HI) were analyzed for snRNP binding. (**B**) Effect of 3′ splice site deletion mutations on snRNP binding. Biotinylated SP6/H$\beta^{\Delta PyAG}$ (ΔPyAG), SP6/H$\beta^{\Delta Py}$ (ΔPy), and SP6/H$\beta^{\Delta AG}$ (ΔAG) (Ruskin and Green, 1985b) were analyzed for snRNP binding. In SP6/H$\beta^{\Delta PyAG}$, the 3′ splice junction and most of the polypyrimidine tract are deleted, but the normal branch point is intact. In SP6/H$\beta^{\Delta Py}$, the polypyrimidine tract is deleted, but the branch point and 3′ splice junction are intact. SP6/H$\beta^{\Delta AG}$ contains a deletion of the four 3′-terminal nucleotides of the intron (IVS1), including the AG dinucleotide at the 3′ splice junction. The snRNP composition of splicing complexes formed using the SP64-HβΔ6/*Bam*HI pre-mRNA in the presence (HβΔ6) or absence (−ATP) of ATP is shown. (**C**) SnRNP composition of partial splicing complexes. The snRNA composition of splicing complexes formed with SP64-HβΔ6 RNAs (extending to the *Bam*HI, *Mbo*II, or to the *Bst*NI site) and with an SP64-HβΔ6 RNA lacking the 5′ splice site (Δ5′/*Bam*HI) was determined after incubation in nuclear extract for 30 min under splicing conditions (ATP: +) or the absence of ATP (ATP: −).

assembly and to gain further insight into the composition and structure of splicing complexes, we have analyzed these complexes both in the crude nuclear extract and after their fractionation by sucrose gradient sedimentation. We present evidence that U1 snRNP is present in complexes at all stages of assembly, but in the larger complexes is 'loosely' bound and therefore can be dislodged by various experimental treatments. In addition, we examine the biochemical and sequence requirements for the interactions between specific snRNPs and the pre-mRNA. Based on the combined results of these studies we propose a pathway for the assembly of a functional splicing complex.

## Results

### *Identification of snRNPs in splicing complexes using biotin–avidin affinity chromatography*

To investigate the composition of splicing complexes generated during *in vitro* splicing of an SP6/human β-globin pre-mRNA, we have purified splicing complexes from the crude nuclear extract by biotin–avidin affinity chromatography. A similar strategy has recently been used to analyze sucrose gradient fractionated splicing complexes (Grabowski and Sharp, 1986). $^{32}$P-labelled pre-mRNA was synthesized *in vitro* in the presence of a biotin–UTP analog (biotin-11-UTP). Following incubation of the biotinylated pre-mRNA in the crude nuclear extract, the splicing complexes are selectively recovered on streptavidin immobilized on agarose beads (streptavidin agarose).

Efficient recovery of the pre-mRNA from the crude nuclear extract (>50%) by biotin–streptavidin affinity chromatography requires raising the salt concentration to 300 mM or higher (data not shown) or the addition of heparin (Grabowski and Sharp, 1986; and see below). Presumably, high salt concentrations or heparin remove bound components that mask biotin groups. In the majority of experiments in this report, 500 mM KCl was used for this purpose. Under these conditions, not only are recoveries optimal (>50%), but also non-specific binding (e.g. binding of non-biotinylated RNAs and endogenous snRNPs to streptavidin agarose) is minimal (see for example Figure 1A, control). Previous studies have demonstrated that splicing complexes are relatively resistant to high ionic strength (Grabowski *et al.*, 1985; Bindereif and Green, 1986; but see below).

To identify the snRNPs in splicing complexes, the complexes bound to streptavidin agarose are digested with proteinase K. The associated snRNPs released by the proteinase K treatment are then labeled with $^{32}$P and identified by denaturing gel electrophoresis. When the wild type SP6/β-globin pre-mRNA is incubated for 30 min in the nuclear extract, all five major snRNPs associate with the pre-mRNA (Figure 1A). U1, U2, U4, U5 and U6 snRNAs were identified by several criteria, including (i) their characteristic electrophoretic mobility (compare for example with Lerner and Steitz, 1979), (ii) their immunoprecipitability by anti-trimethylguanosine antibodies (anti-TMG) (Lührmann *et al.*, 1982; Figure 1B), (iii) their partial RNase T1 digestion pattern (data not shown), and (iv) their cleavage by RNase H using snRNA-specific oligonucleotides (data not shown).

The additional prominent RNA species migrating just below U1 snRNA (Figure 1B) is the SP6/β-globin first exon RNA processing product. This assignment is based upon: (i) comigration of this $^{32}$P-end-labeled RNA with the first exon RNA species (Figure 1B), (ii) the absence of a trimethylguanosine cap structure (Figure 1B), and (iii) identification of the 3′-terminal RNase T1 fragment (data not shown). We note that the smaller first exon RNA species is preferentially released, compared to the IVS1-exon 2 RNA species, by proteinase K treatment of streptavidin agarose-bound splicing complexes. In some early experiments, we observed a 3′-end-labeled RNA with a trimethylguanosine cap structure that migrates between U1 and U4 snRNAs (see for example Figure 1B). The variable levels of this RNA species suggest it is a U1 or U2 snRNA degradation product.

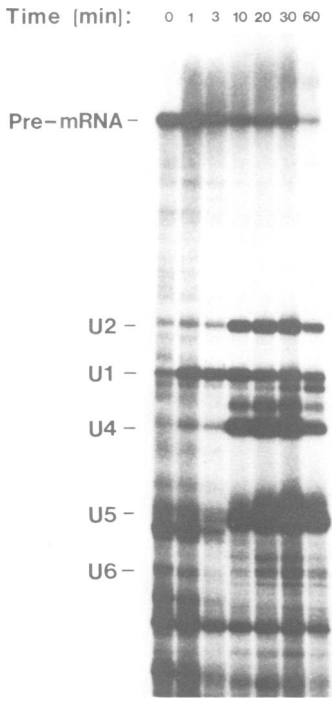


**Fig. 3.** Time course of snRNP binding to SP64-HβΔ6/*Bam*HI pre-mRNA. Aliquots were taken at the indicated times and quickly frozen at −70°C. For the 0 min time point, the components of the splicing reaction were mixed on ice. After thawing the aliquots, snRNP binding was analyzed.

Thus, a minimum of 5 snRNPs (U1, U2, U4, U5 and U6 snRNPS) are components of splicing complexes. Figure 1A demonstrates that all five snRNPs are specifically bound since these snRNPs do not associate with a 516 nucleotide (nt) biotinylated SP64-derived RNA. Binding of all snRNPs except U1 snRNP is ATP dependent (Figure 1A).

### *Sequence requirements for snRNP binding*

Next, we investigated the pre-mRNA sequence requirements for snRNP binding. Specific, efficient snRNP binding requires splice sites since a biotinylated SP6/β-globin cDNA transcript is a poor substrate for snRNP binding (Figure 1A). To determine the role of exon sequences in snRNP binding, we analyzed several SP6/β-globin-derived pre-mRNAs containing IVS1 and various amounts of exons 1 and 2. As shown in Figure 2A, neither shortening the first exon to approximately 20 nt (mini-E1) nor truncating the second exon from 209 nt (HβΔ6/*Bam*HI) to 120, 53 and 24 nt (HβΔ6/*Ban*I, *Xho*II, and *Ava*II, respectively) significantly affects snRNP binding. Thus, only minimal exon sequences are required for efficient binding of U1, U2, U4, U5 and U6 snRNPs. In addition, these experiments suggest that none of the snRNPs specifically interact with exon sequences other than those flanking splice sites.

Next, we analyzed snRNP binding to three mutant RNA substrates that contain small deletions within the polypyrimidine tract and the 3′ splice site (Figure 2B). The 3′ splice site dele-

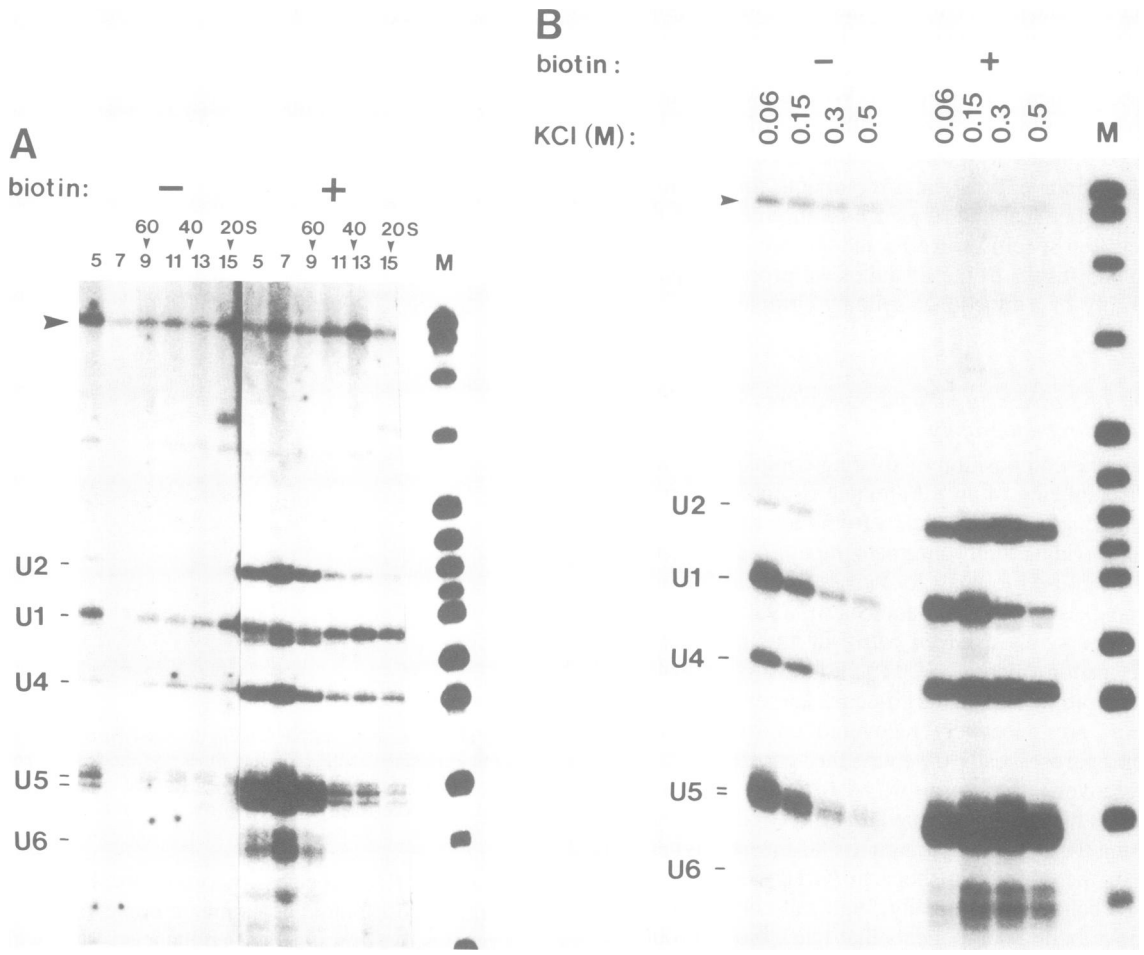


**Fig. 4.** SnRNP composition of sucrose gradient fractionated splicing complexes. Splicing complexes formed using non-biotinylated (biotin: −) and biotinylated (biotin: +) SP64-HβΔ6/*Bam*HI pre-mRNA were fractionated by sucrose gradient sedimentation (60 mM KCl). The positions of pre-mRNA (arrow) and of the snRNAs are indicated on the left. M, $^{32}$P-labeled *Hpa*II-digested pBR322 DNA. (**A**) Identification of snRNPs in splicing complexes. Sucrose gradient-fractioned splicing complexes were analyzed for their snRNP composition by biotin–avidin affinity chromatography (0.5 M KCl). The fractions are numbered 1 through 20 from the bottom to the top of the gradient. The fraction numbers and the sedimentation markers are indicated above the lanes. (**B**) Affinity purification of 60S splicing complex at different ionic strengths. 60S splicing complexes were isolated by sucrose gradient sedimentation at 60 mM KCl (pool of fractions #7–9) and aliquots affinity purified at either 60 mM, 150 mM, 300 mM or 500 mM KCl.

tion mutants bind snRNPs at similar levels; compared to the normal pre-mRNA, U1 snRNP binding is unaffected, U2 snRNP binding is reduced to approximately 40% of normal levels, and U4, U5 and U6 snRNP binding falls to 10–40% of normal levels (Figure 2B).

Finally, we investigated snRNP binding to RNA substrates containing only a 5′ splice site or a branch point/3′ splice site region (Figure 2C). Interestingly, RNAs with only one of these two splicing signals are assembled into partial splicing complexes. An RNA extending 66 nt past the 5′ splice site, but lacking the entire branch point/3′ splice site region and second exon (HβΔ6/*Mbo*II), binds U1 snRNP normally; in contrast, binding of all other snRNPs (U2, U4, U5 and U6 snRNPs) is reduced to low but detectable levels (approximately 10–30% of normal levels). An RNA substrate with a shorter first exon, which lacks both 3′ and 5′ splice sites (HβΔ6/*Bst*NI), does not bind any snRNP. Conversely, an RNA substrate lacking the 5′ splice site but containing the branch point/3′ splice site region (Δ5′/*Bam*HI), forms complexes containing U2 snRNP (50 to 100% of normal levels) and low levels of U4, U5 and U6 snRNPs (approximately 10–30% of normal levels). Significantly, assembly of U2, U4, U5 and U6 snRNPs into all partial splicing complexes requires ATP.

*Ordered snRNP binding during splicing complex assembly*

To determine the assembly pathway of a functional splicing complex, we analyzed the time course of snRNP binding (Figure 3). Binding of U1 snRNP is detected immediately (on ice, no incubation of 30°C) and reaches maximal levels after a 1 min incubation at 30°C. U2, U4, U5 and U6 snRNPs all bind with identical kinetics; these snRNPs first associate with the pre-mRNA after 10 min and reach maximal levels by 30 min. At 60 min, when a substantial portion of the pre-mRNA has undergone 5′ splice site cleavage, the levels of bound snRNPs all decrease dramatically.

*Identification of snRNPs in sucrose gradient fractionated splicing complexes*

Our experiments using crude nuclear extracts identify the snRNPs associated with all splicing complexes. We next analyzed the snRNP composition of complexes at various stages of assembly. In these experiments splicing complexes are fractionated by sucrose gradient sedimentation and then affinity purified. Figure 4A shows the analysis of splicing complexes fractionated in a sucrose gradient containing 60 mM KCl and then affinity purified at 500 mM KCl. Under these conditions complexes from 20S through 40S contain predominantly U1 snRNP, whereas the 60S

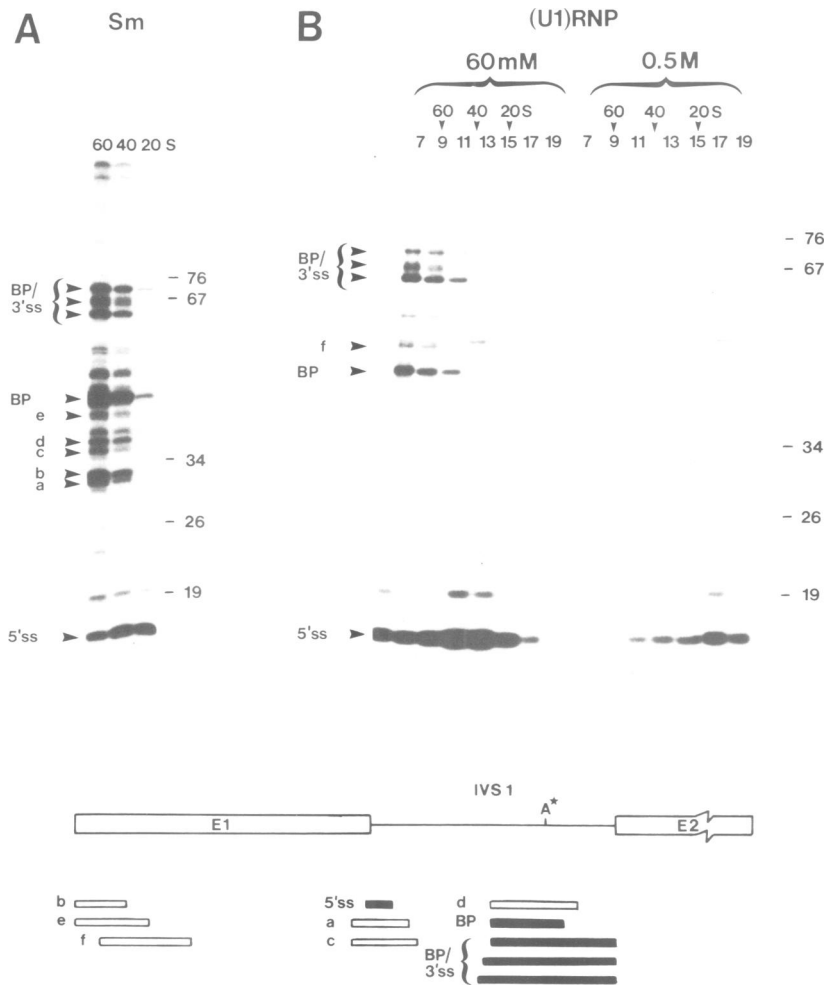


**Fig. 5.** Mapping pre-mRNA−snRNP contacts in splicing complexes. Pre-mRNA−snRNP contacts in sucrose gradient fractionated splicing complexes were mapped by RNase T1 protection-immunoprecipitation analysis. Analyzed RNA fragments are indicated by arrows on the left of each panel (major protected RNA fragments: 5′ss, 5′ splice site region; BP, branch point region; BP/3′ss, branch point/3′ splice site region; and minor protected RNA fragments by lower-case letters). The snRNP binding sites on the pre-mRNA (E1, exon 1; IVS1, intervening sequence 1; E2, exon 2; A*, branch point) are summarized schematically below the panels (major and minor protected RNA fragments denoted by closed and open boxes, respectively). (**A**) Sm-type snRNPs. Splicing complexes were fractionated in sucrose gradients containing 60 mM KCl. SnRNP contacts of the Sm-type (U1, U2, U4, U5 and U6 snRNPs) were mapped in splicing complexes from the 60S (fractions #8−10), 40S (fractions #11−13), and 20S (fractions #14−16) regions (indicated above the lanes). (**B**) U1 snRNP. Splicing complexes were fractionated in sucrose gradients containing 60 mM or 0.5 M KCl. U1 snRNP contacts were mapped using gradient fractions as indicated above the lanes (numbered 1 through 20 from the bottom to the top of the gradient).

splicing complex contains U2, U4, U5 and U6 snRNPs, and low levels of U1 snRNP.

Previous immunoprecipitation studies (Grabowski *et al.*, 1985; Bindereif and Green, 1986) and our RNase protection experiments (see below) indicate that the 60S splicing complex contains U1 snRNP-specific determinants. Therefore, we suspected that our failure to detect U1 snRNP in the affinity purified 60S complex was due to the high salt treatment. To test this prediction, 60S splicing complexes were isolated by sucrose gradient sedimentation at 60 mM KCl and affinity purified at either 60 mM, 150 mM, 300 mM or 500 mM KCl (Figure 4B). At 60 mM KCl, specific binding is obscured by the high background levels of snRNP binding to the streptavidin agarose. At 150 mM KCl and above, however, background levels are sufficiently low to detect readily specific snRNP binding. Strikingly, when the 60S complex is affinity purified at 150 mM KCl, significant levels of U1 snRNP are detectable. But U1 snRNP levels decrease dramatically when 300 mM KCl or 500 mM KCl are used for affinity purification. In contrast, the U2, U4, U5 and U6 snRNP levels remain essentially unchanged at 150 mM, 300 mM and 500 mM KCl. We estimate that at 150 mM KCl, the relative molar amounts of U1/U2/U4/U5/U6 snRNPs in the 60S complex are approximately 0.5/1/1/1/1.

### *Mapping snRNPs in sucrose gradient fractionated splicing complexes*

We next mapped snRNP-pre-mRNA contacts in sucrose gradient purified splicing complexes (Figure 5). The complexes were digested with RNase T1, the RNase T1-resistant fragments immunoprecipitated with anti-snRNP-specific antibodies and identified (Black *et al.*, 1985). The antiserum used was either against all Sm-type snRNPs (U1, U2, U4, U5 and U6 snRNPs; anti-Sm) or against only U1 snRNP [anti-(U1)RNP]. The presence of specific snRNPs can be correlated with the corresponding RNase T1-resistant fragments, thereby mapping snRNPs to discrete pre-mRNA regions.

RNase T1 digestion of the 20S complex generates a characteristic 15 nt fragment that maps to the 5′ splice site and

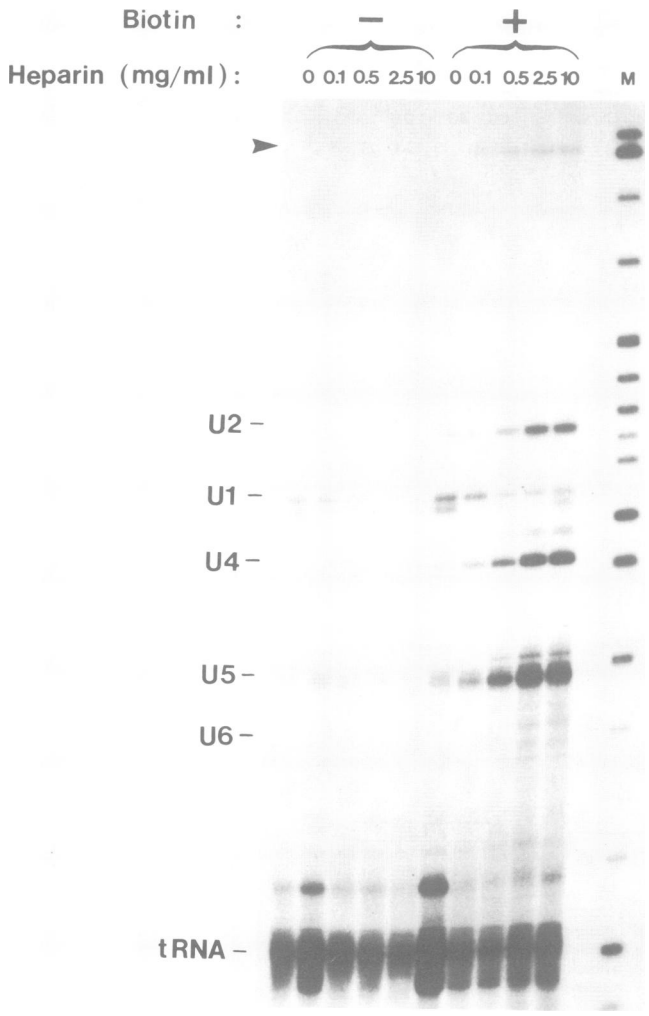


**Fig. 6.** The effect of heparin on snRNP binding. Non-biotinylated (biotin: −) and biotinylated (biotin: +) SP64-Hβ$\Delta$6/*Bam*HI pre-mRNAs were spliced *in vitro* for 20 min, followed by the addition of heparin to the concentration indicated above each lane and incubation continued for 10 min at 30°C. After the addition of an equal volume of SB buffer (10 mM Hepes, pH 8.0, 3 mM $MgCl_2$, 1 mM DTT, and KCl to a final concentration of 0.1 M), splicing complexes were affinity purified and analyzed for snRNP binding. The snRNAs, tRNA and the pre-mRNA (arrow) are indicated on the left. M, $^{32}$P-labeled *Hpa*II-digested pBR322 DNA.

is immunoprecipitated by both Sm- and U1(RNP)-specific antibodies (see Black *et al.*, 1985). Thus, U1 snRNP, which is the only snRNP present in the 20S complex (Figure 4A), is specifically bound to the 5′ splice site, as expected. In the 60S complex, the major RNase T1-resistant fragments map to the branch point/3′ splice site region and to the 5′ splice site (Figure 5). Thus, protection of the branch point/3′ splice site region is due to the additional binding of U2, U4, U5 and U6 snRNPs (and see below). Significantly, the branch point/3′ splice site fragments derived from the 60S complex can be immunoprecipitated by both anti-Sm and anti-U1 snRNP antibodies. Furthermore, RNase T1-resistant fragments larger than 15 nt, which map to the 5′ splice site (referred to as extended 5′ splice site fragments), are unique to the 60S complex. Finally, we note that a region located near the 5′ end of the pre-mRNA is also bound to both Sm- and U1(RNP)-specific determinants.

The RNase T1 protection analysis independently confirms that high salt selectively removes U1 snRNP from the 60S complex. At 500 mM KCl the mature splicing complex sediments at approximately 40S (Bindereif and Green, 1986). In contrast to the 60S complex found at 60 mM KCl, this 40S complex contains a very low level of U1 snRNP determinants at the 5′ splice site (Figure 5B), although normal levels of Sm determinants are bound to the branch point (data not shown). Only in very small complexes (approximately 10S) is the 5′ splice site efficiently protected from RNase T1 digestion. Thus, high ionic strength selectively removes U1 snRNP from the 60S complex. In the smaller complexes, the U1 snRNP binding may be salt stable and can therefore be detected by affinity chromatography (Figure 4A) and RNase protection analysis (Figure 5B) in 500 mM KCl.

*Affinity purification of splicing complexes after heparin treatment*

In a previous study, biotin-streptavidin affinity chromatography was used to determine the snRNP composition of splicing complexes formed using an adenovirus major late pre-mRNA (Grabowski and Sharp, 1986). In this case, splicing complexes were incubated with heparin prior to sucrose gradient fractionation, resulting in discrete 35S, 25S and 15S heparin-resistant complexes. These heparin-resistant complexes contain U2, U4, U5 and U6 snRNPs (35S complex), U2 snRNP only (25S complex), or no snRNP (15S complex). Thus, in contrast to our results, U1 snRNP was not detected in any complex (Grabowski and Sharp, 1986).

Since we found that U1 snRNP in the 60S complex is removed by high salt (see above), we postulated that it may also be heparin labile. To test this possibility, splicing complexes were affinity purified from the crude nuclear extract using various concentrations of heparin. Figure 6 demonstrates that at least 2.5 mg/ml heparin is required for efficient affinity purification of splicing complexes from the crude nuclear extract. Significantly, splicing complexes affinity purified after heparin treatment lack U1 snRNP (Figure 6) in contrast to splicing complexes affinity purified using high salt (Figure 1A).

The different pre-mRNA substrates used in our experiments and in the previous study (Grabowski and Sharp, 1986) may also have contributed to the different results obtained. To address this possibility, complexes formed with the human β-globin pre-mRNA were treated with heparin and fractionated by sucrose gradient sedimentation. Two distinct heparin-resistant complexes were obtained, neither of which contained U1 snRNP. The 25S complex contains only U2 snRNP whereas the 35S complex contains equimolar amounts of U2, U4, U5 and U6 snRNPs (Figure 7A). (The low level of U5 snRNP detectable in the 25S region is due to minor contamination by the 35S complex.) Thus, after heparin treatment, corresponding splicing complexes are formed with the human β-globin and adenovirus major late pre-mRNAs.

*The U4, U5 and U6 snRNPs are primarily bound by snRNP–snRNP interactions*

The availability of two discrete splicing complexes differing only by the presence or absence of U4, U5 and U6 snRNPs allowed us to localize these snRNPs. The heparin-resistant 35S and 25S complexes were digested with RNase T1 and the resulting RNA fragments immunoprecipitated using anti-Sm, anti-U1/U2, and anti-(U1)RNP antibodies (Figure 7B). Consistent with the results described above, U1 snRNP is removed by the heparin pretreatment; in both the 35S and 25S heparin-resistant complexes, the 5′ splice site is not protected from RNase T1 digestion. Strikingly, the RNase protection patterns of the heparin-resistant 35S complex (U2, U4, U5 and U6 snRNPs) and 25S complex (U2 snRNP only) are nearly identical. In both

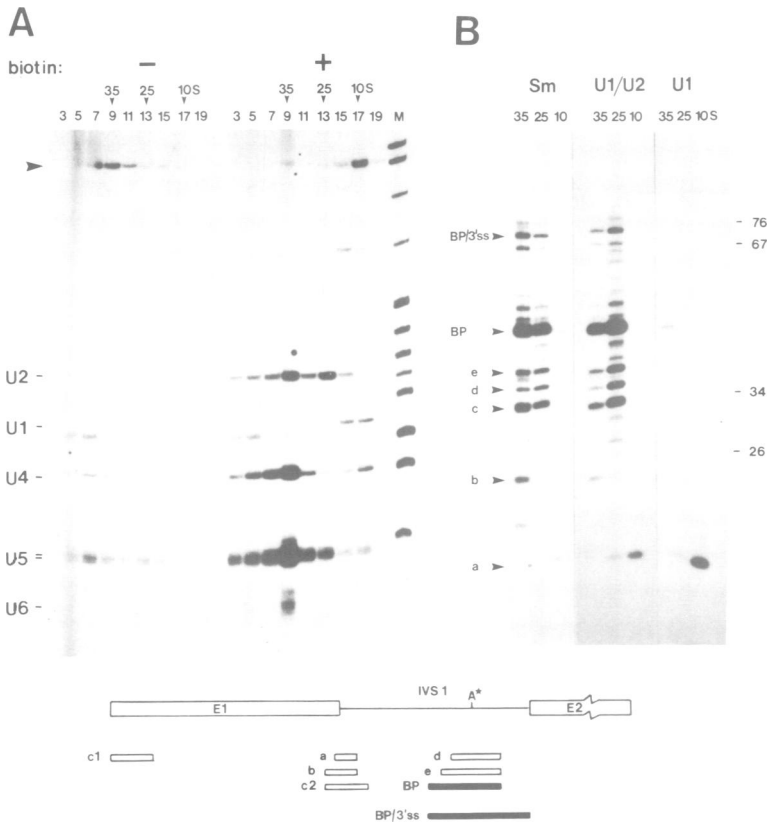


**Fig. 7.** Identification of snRNPs and mapping of pre-mRNA−snRNP contacts in heparin-resistant splicing complexes. (**A**) Identification of snRNPs. Heparin-resistant splicing complexes formed using non-biotinylated (biotin: −) and biotinylated (biotin: +) SP64-H$\beta\Delta$6/*Bam*HI pre-mRNAs were fractionated by sucrose gradient sedimentation (60 mM KCl) and analyzed for their snRNP composition by biotin−avidin affinity chromatography (100 mM KCl). The fractions are numbered 1 through 20 from the bottom to the top of the gradient. The fraction numbers and the sedimentation markers are indicated above the lanes, the snRNAs and the pre-mRNA (arrow) on the left. (**B**) Mapping of pre-mRNA−snRNP contacts. Heparin-resistant splicing complexes were fractionated by sedimentation through sucrose gradients containing 60 mM KCl. The fractions are numbered 1 through 20 from the bottom to the top of the gradient. Fractions containing heparin-resistant splicing complexes of approximately 35S (#9/10), 25S (#13/14), and 10S (#17/18) were pooled and used in RNase T1 protection-immunoprecipitation assays with antisera against Sm-type snRNPs (anti-Sm), U1 and U2 snRNPs (anti-U1/U2), and against U1 snRNP (anti-U1) (indicated above the lanes). Analyzed RNA fragments are indicated by arrows on the left of each panel (major protected RNA fragments: BP, branch point region; BP/3′ss, branch point/3′ splice site region; and minor protected RNA fragments by lower-case letters). The mapping analysis of snRNP binding sites on the pre-mRNA (E1, exon 1; IVS1, intervening sequence 1; E2, exon 2; A*, branch point) is schematically summarized below the panels (major and minor protected RNA fragments indicated by closed and open boxes, respectively).

complexes the RNase T1-resistant fragments map to the branch point region. Therefore, the U4, U5 and U6 snRNPs do not significantly contribute to the protection of the pre-mRNA from RNase digestion, suggesting that these snRNPs do not contact the pre-mRNA. Since the protection pattern using anti-Sm and anti-U1/U2 antibodies is identical, the RNase T1 protection can be attributed entirely to U2 snRNP binding. In the 35S complex, there is an additional, weakly protected fragment that is immunoprecipitated by both anti-Sm and anti-U1/U2 antibodies and maps to the 5′ splice site.

In summary, these results imply that in the 35S complex U4, U5 and U6 snRNPs associate indirectly with the pre-mRNA, primarily through interactions with bound U2 snRNP. Furthermore, an snRNP(s) in the heparin-resistant 35S complex contacts the 5′ splice site. This additional contact may be related to the extended 5′ splice site protection in the 60S complex (see Figure 5A). Our results do not unambiguously identify the snRNP(s) that mediates this additional 5′ splice site interaction. However, the extended 5′ splice site fragment is immunoprecipitated by the anti-U1/U2 antibody, implicating the U2 snRNP.

## Discussion

In this report pre-mRNA−snRNP interactions have been analyzed by two approaches. First, the specific snRNPs associated directly or indirectly with the pre-mRNA were identified using biotin−avidin affinity chromatography. Second, the pre-mRNA regions bound by snRNPs were delineated by RNase T1 protection analysis. The affinity chromatography and RNase protection methods are complementary; one identifies the factors present in splicing complexes while the other maps interactions between these factors and the pre-mRNA.

In correlating the results obtained by these two approaches, we note that, in contrast to RNase T1 protection analysis, affinity chromatography is performed under ionic conditions different from the splicing reaction. Efficient affinity purification of splicing complexes requires elevated salt concentrations (this study) or the addition of heparin (Grabowski and Sharp, 1986; this study). Presumably, salt or heparin removes bound components that mask biotin groups. Thus, the absence of a component from an affinity-purified splicing complex is not proof that the component is not actually a constituent of the splicing complex. Based upon the results of this and previous studies, a model for

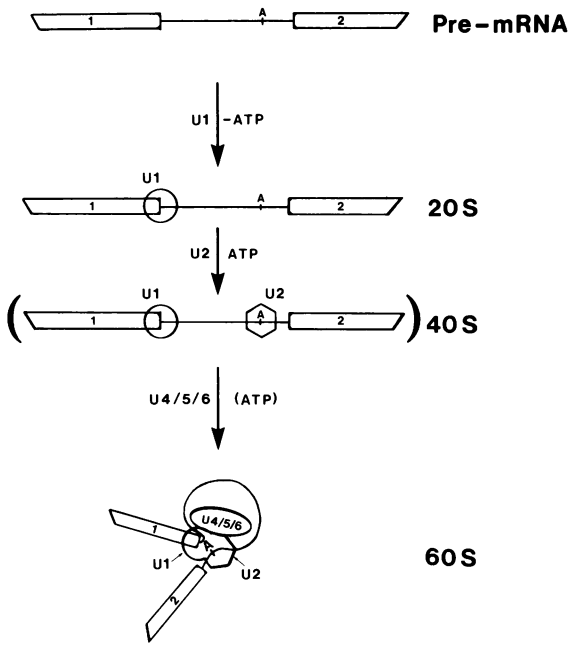


**Fig. 8.** Proposed pathway of snRNP binding during splicing complex assembly. A pathway for snRNP binding during splicing complex assembly is schematically outlined. Direct experimental evidence has been presented for the composition and snRNP arrangement in the 20S and 60S complexes. Steps enclosed by parentheses indicate a lack of direct experimental evidence. This proposed pathway differs in several important aspects from previous models (Konarska and Sharp, 1986; Chabot and Steitz, 1987; Sharp, 1987; Maniatis and Reed, 1987). In particular, note the order of snRNP binding, the presence of U1 snRNP in the 60S complex, and that U4, U5 and U6 snRNPs interact with U1 and U2 snRNPs rather than with the pre-mRNA.

splicing complex assembly is proposed and discussed below (Figure 8).

*Biochemical and sequence requirements for snRNP binding*

U1 is the only snRNP that efficiently binds to the pre-mRNA in the absence of ATP. The ATP-independent binding of U1 snRNP is consistent with previous studies (Black *et al.*, 1985) and reflects the fact that U1 snRNP binds primarily by intermolecular base-pairing between U1 snRNA and the 5′ splice site (Zhuang and Weiner, 1986 and references therein). The ATP-dependence of U2 snRNP binding is also consistent with previous reports (Black *et al.*, 1985; Ruskin and Green, 1985a) and possible explanations have been discussed (Ruskin and Green, 1985a). However, the ATP requirement for the binding of U4, U5 and U6 snRNPs was previously unknown. Based upon our combined data, the simplest explanation for the ATP requirement of U4, U5 and U6 snRNP binding is that these snRNPs interact with bound U2 snRNP (see below).

It is particularly noteworthy that binding of U5 snRNP is ATP dependent. The 3′ splice site interacts with a micrococcal nuclease-resistant snRNP, which has been suggested to be U5 snRNP (Chabot *et al.*, 1985). Our data do not support this suggestion; binding of U5 snRNP is ATP dependent (Figure 1A), whereas ATP is not required for the interaction of an snRNP with the 3′ splice site (Chabot *et al.*, 1985). However, we cannot rule out that U5 snRNP binds initially in an ATP-independent manner forming a salt- and heparin-labile complex, which in the presence of ATP is converted to a salt- and heparin-stable complex.

Several other observations also indicate that U5 snRNP does not bind directly to the 3′ splice site. First, U5 snRNP associates poorly with RNA substrates that contain an intact 3′ splice site but lack a 5′ splice site, suggesting that the 3′ splice site is not the direct binding site for U5 snRNP. Unlike U5 snRNP, U2 snRNP efficiently binds to this mutant RNA substrate. Thus, U2 snRNP apparently can bind to the pre-mRNA in the absence of bound U5 snRNP. Second, our nuclease-protection data (see below) suggest that U5 snRNP does not directly contact the 3′ splice site.

*SnRNP contacts in the splicing complex*

Previous studies have established that U1 and U2 snRNPs bind to the 5′ splice site and the branch point, respectively (Black *et al.*, 1985). Although U4, U5 and U6 snRNPs are components of splicing complexes, our nuclease-protection data suggest that these snRNPs do not contact the pre-mRNA; instead we propose that U4, U5 and U6 snRNPs interact primarily with bound U2 snRNP and probably bound U1 snRNP. U1 snRNP facilitates the stable assembly of U4, U5 and U6 snRNPs into splicing complexes; compared to the wild type pre-mRNA, substrates lacking a 5′ splice site bind U4, U5 and U6 snRNPs inefficiently. The conclusion that U4, U5 and U6 snRNPs primarily contact the U2 snRNP is consistent with several experimental observations, including: (i) the kinetics of snRNP binding (Figure 3), (ii) the ATP-dependent binding of U4, U5 and U6 snRNPs, as well as that of U2 snRNP (Figure 1A) and (iii) the effect of 3′ splice site mutations that decrease both U2 snRNP binding and U4, U5 and U6 snRNP binding (Figure 2B).

Substrates containing either a 5′ splice site or a 3′ splice site/branch point region form partial splicing complexes. This probably reflects the fact that U1 and U2 snRNPs initially bind independently of each other to separate pre-mRNA sites that are subsequently brought into proximity by snRNP–snRNP interactions. U4, U5 and U6 snRNPs may mediate this 'bridging' process by simultaneously interacting with bound U2 and U1 snRNPs. In the absence of a 5′ splice site, U4, U5 and U6 snRNPs associate at low efficiency with bound U2 snRNP. In the absence of a 3′ splice site/branch point region, U2, U4, U5 and U6 snRNPs associate at a low efficiency with bound U1 snRNP. However, both the 5′ splice site and 3′ splice site/branch point region are required for efficient U4, U5 and U6 snRNP binding. In all of our experiments, U4, U5 and U6 snRNPs behave similarly, consistent with the possibility that they act in concert.

We were surprised to find U2 snRNP in splicing complexes formed using RNA substrates that contain 3′ splice site mutations. Previous studies have demonstrated that the branch point of such substrates is not protected from RNase A digestion (Ruskin and Green, 1985a), indicating that U2 snRNP is not bound tightly to its cognate site. We suggest that in these partial splicing complexes, U2 snRNP interacts primarily with U1 snRNP bound at the 5′ splice site. Thus, truncation of the 5′ splice site abolishes U1 snRNP binding as well as the low efficiency binding of U2, U4, U5 and U6 snRNPs (Figure 2C).

*An ordered pathway of snRNP binding*

Both the time course of snRNP binding and the snRNP composition of gradient fractionated splicing complexes suggest that splicing complexes are assembled in an ordered pathway (Figure 8). First, U1 snRNP binds to the 5′ splice site forming a complex of approximately 20S. Second, U2 snRNP binds to the branch point of the 20S complex forming a complex with an estimated size of approximately 40S. Third, U4, U5 and U6 snRNPs associate with the 40S complex to form the functional 60S com-

plex, the actual splicing substrate. This model represents the preferred order of snRNP binding in the nuclear extract and does not necessarily imply an obligatory assembly pathway. For example, U2 snRNP can efficiently and tightly bind to the branch point in the absence of a 5′ splice site (Ruskin and Green, 1985a; Figure 2C).

We note that no direct evidence has been provided for the precursor-product relationships suggested above. For example, it is conceivable that the 20S complex (U1 snRNP) or the 40S complex (U1 and U2 snRNPs) are dead-end products and not intermediates. Kinetic evidence for a stepwise assembly of splicing complexes has been provided by sucrose gradient sedimentation experiments (Frendewey and Keller, 1985) and the analysis of splicing complexes on non-denaturing gels (Pikielny *et al.*, 1986; Konarska and Sharp, 1986).

Direct evidence for the snRNP composition of 20S and 60S complexes is provided by biotin−streptavidin affinity chromatography. In contrast, the 40S complex containing only U1 and U2 snRNPs (Figure 8) has not been detected directly. Although large amounts of $^{32}$P-labeled RNA substrate sediment in the 40S region, our previous study suggested that most of these complexes are non-productive and result from interactions of non-specific RNA binding factors with the pre-mRNA (Bindereif and Green, 1986). We postulate the existence and composition of the 40S complex (U1/U2 snRNPs) based upon the following considerations. U1 snRNP can be detected in 20S through 60S complexes; U2 snRNP, however, can be detected only in 60S complexes. Although U4, U5, U6 snRNPs appear to interact with bound U2 snRNP, their binding cannot be kinetically resolved from U2 snRNP binding (Figure 3). But U2 snRNP binding can be resolved from U4, U5 and U6 snRNP binding using an RNA substrate that lacks the 5′ splice site and therefore binds U4, U5 and U6 snRNPs inefficiently. We suggest that with the wild type pre-mRNA, the steady-state level of the U1/U2 snRNP complex (40S) is low due to the rapid binding of U4, U5 and U6 snRNPs. Thus, under the standard *in vitro* splicing conditions, binding of U2 snRNP may be the rate-limiting step in assembly of a functional splicing complex.

The 60S splicing complex contains U1, U2, U4, U5 and U6 snRNPs. Consistent with the previous study (Grabowski and Sharp, 1986), U2, U4, U5 and U6 snRNPs are present in approximately unit stoichiometry. Moreover, the relative molar amounts of U2, U4, U5 and U6 snRNPs do not change under different ionic conditions. In contrast, raising the ionic strength during affinity purification results in a relative decrease in U1 snRNP recovery (Figure 4B). RNase T1 protection experiments in this and another recent study (Chabot and Steitz, 1987) confirm that U1 snRNP antigens are present in the 60S complex.

Several observations indicate that the ATP-dependent binding of U2 and/or U2, U4, U5, U6 snRNPs alters the ribonucleoprotein structure at the 5′ splice site. First, in a time- and ATP-dependent manner, the 5′ splice site becomes resistant to oligonucleotide-directed RNase H cleavage (Ruskin and Green, 1985a). Second, RNase T1 digestion of the 60S but not 20S complexes generates extended 5′ splice site fragments. This extended 5′ splice site protection probably results from conformational changes due to the additional binding of U2 and/or U4, U5 and U6 snRNPs. These conformational changes may destabilize U1 snRNP binding in the 60S complex by, for example, disrupting base-pairing between U1 snRNA and the 5′ splice site (Zhuang and Weiner, 1986). Further studies are necessary to understand how structural alterations mediated by snRNP−snRNP interactions contribute to splice site cleavage mechanisms.

## Materials and methods

### *Materials*

SP6 RNA polymerase, RNasin, DNase I, and restriction enzymes were from Promega Biotec or New England Biolabs, RNase T1 from Calbiochem, RNase A from Boehringer Mannheim, and GpppG from Pharmacia. Protein A−Sepharose and T4 RNA ligase were purchased from Pharmacia, streptavidin agarose and biotin-11-UTP from BRL. [$\alpha$-$^{32}$P]UTP (410 Ci/mmol) was purchased from Amersham. [5′-$^{32}$P]pCp was prepared from cytidine 3′-monophosphate (Sigma) and [$\gamma$-$^{32}$P]ATP (>6000 Ci/mmol; New England Nuclear) as described (England *et al.*, 1980).

### *Plasmids, SP6 transcription and pre-mRNA splicing reactions*

The following DNA templates have been previously described: SP64-H$\beta\Delta$6 (Krainer *et al.*, 1984), SP64 (Melton *et al.*, 1984), SP64-H$\beta\Delta$-IVS1,2 (termed 'H$\beta$cDNA' in Figure 1A) (Krainer *et al.*, 1984), SP6/H$\beta^{\Delta PyAG}$ (Ruskin and Green, 1985b), SP6/H$\beta^{\Delta Py}$ (Ruskin and Green, 1985b), SP6/H$\beta^{\Delta AG}$ (Ruskin and Green, 1985b). SP64-H$\beta$mini-E1 (termed 'mini-E1' in Figure 2A) was derived from SP64-H$\beta$IVS1 (Ruskin *et al.*, 1984) by adding the *Acc*I−*Bam*HI fragment (positions +284 to +477, Lawn *et al.*, 1980) to SP64−H$\beta$IVS1 to restore the second exon sequences. $\Delta$5′ was contructed by deleting SP64-H$\beta$mini-E1 linearized at the *Hin*dIII site with *Bal*31 nuclease. A *Hin*dIII linker was ligated to the deletion end-point and the *Hin*dIII−*Bam*HI fragment recloned between the *Hin*dIII and *Bam*HI sites of pSP64. The first 12 nucleotides of IVS1 are deleted in $\Delta$5′.

High-specific activity, $^{32}$P-labeled RNA ($5 \times 10^7$ c.p.m./$\mu$g) was synthesized as previously described (Bindereif and Green, 1986). Low-specific activity, $^{32}$P-labeled RNA ($2 \times 10^6$ c.p.m./$\mu$g) was synthesized in 25 $\mu$l-reactions containing 2 $\mu$g DNA template, 40 mM Tris−HCl (pH 7.5), 6 mM $MgCl_2$, 2 mM spermidine, 15 mM DTT, 0.4 $\mu$l RNasin, 50 $\mu$M GTP, 1 mM GpppG, 500 $\mu$M of each of the unlabeled nucleoside triphosphates, [$\alpha$-$^{32}$P]UTP (25 $\mu$Ci), and 20 units SP6 RNA polymerase.

Unless otherwise specified, *in vitro* splicing reactions were carried out for 30 min using 30−90 ng of SP64-H$\beta\Delta$6/*Bam*HI substrate per 1 × reaction as previously described (Krainer *et al.*, 1984; Ruskin *et al.*, 1984), without the addition of polyvinylalcohol.

### *Biotin−streptavidin affinity chromatography*

Biotinylated RNA was synthesized by including biotin-11-UTP (15% of total UTP) in the standard SP6 transcription reaction. The incorporation of biotin-11-UTP under these conditions neither affected the mobility of the biotinylated RNA in denaturing gels or its splicing efficiency, nor did it alter splicing complex formation (data not shown).

After incubation of biotinylated RNA in nuclear extract under standard conditions, an equal volume of SB buffer (10 mM Hepes, pH 8.0, 3 mM $MgCl_2$, 1 mM DTT, and KCl to a final concentration of 0.5 M) was added on ice. The splicing reaction mixture was then centrifuged at 12 000 × *g* for 5 min at 4°C, and to the supernatant 40 $\mu$l of a 1:1 suspension of streptavidin agarose beads in NET-2 buffer (50 mM Tris−HCl pH 7.9, 0.05% Nonidet P-40 [vol/vol], 0.5 mM DTT) containing 0.5 M KCl was added. The binding reaction proceeded for 2 h at 4°C with agitation, the streptavidin agarose beads were pelleted in a microfuge (10 s), and washed four times with 0.8 ml each of NET-2 buffer (0.5 M KCl) over a period of 2 h. Bound snRNAs were released from the streptavidin agarose by proteinase K treatment, ethanol-precipitated with 2 $\mu$g of DNA carrier, 3′-end-labeled with [5′-$^{32}$P]pCp and T4 RNA ligase (England *et al.*, 1980), analyzed on a 9% denaturing polyacrylamide gel and detected by autoradiography.

Fractionation of splicing complexes in sucrose gradients containing 60 mM KCl is as previously described (Bindereif and Green, 1986), except that centrifugation was in an SW40 rotor at 40 000 r.p.m. for 4 h. 40 $\mu$l of streptavidin agarose suspension (in NET-2 buffer, KCl concentration of the gradient fraction) were added to 1-ml gradient fractions after adjustment of the KCl concentration as indicated in the figure.

To fractionate heparin-resistant splicing complexes, the splicing reaction mixture was incubated at 30°C for 20 min followed by the addition of heparin to a final concentration of 5 mg/ml and continued incubation at 30°C for 10 min. Heparin-resistant splicing complexes were sedimented for 5 h in sucrose gradients containing 60 mM KCl.

Relative amounts of snRNPs in 60S splicing complexes were estimated by comparing the autoradiographic signals of labeled snRNAs and correcting for their labeling efficiencies. Labeling efficiencies of individual snRNAs were determined by comparing the ethidium bromide staining intensities of the snRNAs with the autoradiographic signals after 3′-end-labeling (data not shown). Relative amounts of snRNPs in affinity purified splicing complexes were determined by densitometric scanning of the autoradiograms.

### *RNase T1 protection-immunoprecipitation assays*

Anti-Sm and anti-(U1)RNP sera were obtained from the Center for Disease Control (Atlanta, Georgia). Anti-U1/U2-snRNP antiserum (Reeves *et al.*, 1986) was kindly

provided by Dr Reeves. These sera immunoprecipitated the snRNPs expected from their specificity (data not shown).

Sucrose gradient fractions were pooled as indicated, added to an antiserum–RNasin mixture (2 μl antiserum and 10 μl RNasin/ml gradient fraction) and incubated on ice for 30 min. Gradient fractions containing 60 mM KCl (Figures 5, 7B) were used undiluted whereas gradient fractions containing 0.5 M KCl (Figure 5B) were diluted to 0.25 M KCl with SB buffer (10 mM Hepes, pH 8.0, 3 mM $MgCl_2$, 1 mM DTT). RNase T1 was added (40 units/ml for anti-Sm and anti-U1/U2 snRNP antisera; 20 units/ml for anti-U1 antiserum) and incubated for 30 min at 30°C. The mixture was placed on ice and 50 μl of a 1:1 suspension of protein A–Sepharose CL-4B (7.5 mg; Pharmacia) in NET-2 buffer (50 mM Tris–HCl pH 7.9; 150 mM NaCl; 0.05% Nonidet P-40 vol/vol; 0.5 mM DTT) was added. After incubation for 30 min at 4°C with agitation, the immunoprecipitate was pelleted (10 s in a microfuge) and washed three times with 0.8 ml of NET-2 buffer. RNA was purified from the immunoprecipitate and analyzed on a 12% denaturing polyacrylamide gel. RNA analysis was performed as previously described (Ruskin *et al.*, 1984).

## Acknowledgements

We are grateful to Dr W.Reeves for providing the anti-U1/U2 and to Dr R.Lührmann for the anti-trimethylguanosine antibodies. We acknowledge the excellent technical assistance of M.McCaffrey and J.Grobholz and thank members of this laboratory and M.Rosbash's laboratory for critical comments on the manuscript. A.B. was supported by a postdoctoral fellowship from the Deutsche Forschungsgemeinschaft. This work was supported by grants from the National Institutes of Health and The Chicago Community Trust/Searle Scholars Program to M.R.G.

## References

Berget,S.M. and Robberson,B.L. (1986) *Cell*, **46**, 691–696.
Bindereif,A. and Green,M.R. (1986) *Mol. Cell. Biol.*, **6**, 2582–2592.
Black,D.L., Chabot,B. and Steitz,J.A. (1985) *Cell*, **42**, 737–750.
Black,D.L. and Steitz,J.A. (1986) *Cell*, **46**, 697–704.
Brody,E. and Abelson,J. (1985) *Science*, **228**, 963–967.
Chabot,B., Black,D.L., LeMaster,D.M. and Steitz,J.A. (1985) *Science*, **230**, 1344–1349.
Chabot,B. and Steitz,J.A. (1987) *Mol. Cell. Biol.*, **7**, 281–293.
Choi,Y.D., Grabowski,P.J., Sharp,P.A. and Dreyfuss,G. (1986) *Science*, **231**, 1534–1539.
England,T.E., Bruce,A.G. and Uhlenbeck,O.C. (1980) In Grossman,L. and Moldave,K. (eds), *Methods in Enzymology*. Vol. 65, Academic Press, New York, pp. 65–74.
Frendewey,D. and Keller,W. (1985) *Cell*, **42**, 355–367.
Furneaux,H.M., Perkins,K.K., Freyer,G.A., Arenas,J. and Hurwitz,J. (1985) *Proc. Natl. Acad. Sci. USA*, **82**, 4351–4355.
Grabowski,P.J., Seiler,S.R. and Sharp,P.A. (1985) *Cell*, **42**, 345–353.
Grabowski,P.J. and Sharp,P.A. (1986) *Science*, **233**, 1294–1299.
Green,M.R. (1986) *Annu. Rev. Genet.*, **20**, 671–708.
Hernandez,N. and Keller,W. (1983) *Cell*, **35**, 89–99.
Kaltwasser,E., Spitzer,S.G. and Goldenberg,C.J. (1986) *Nucleic Acids. Res.*, **14**, 3687–3701.
Konarska,M.M. and Sharp,P.A. (1986) *Cell*, **46**, 845–855.
Krainer,A.R., Maniatis,T., Ruskin,B. and Green,M.R. (1984) *Cell*, **36**, 993–1005.
Krainer,A.R. and Maniatis,T. (1985) *Cell*, **42**, 725–736.
Krämer,A., Keller,W., Appel,B. and Lührmann,R. (1984) *Cell*, **38**, 299–307.
Lawn,R.M., Efstratiadis,A., O'Connell,C. and Maniatis,T. (1980) *Cell*, **21**, 647–651.
Lerner,M.R. and Steitz,J.A. (1979) *Proc. Natl. Acad. Sci. USA*, **76**, 5495–5499.
Lührmann,R., Appel,B., Bringmann,P., Rinke,J., Reuter,R., Rothe,S. and Bald,R. (1982) *Nucleic Acids. Res.*, **10**, 7103–7113.
Maniatis,T. and Reed,T. (1987) *Nature*, **325**, 673–678.
Melton,D.A., Krieg,P.A., Rebagliati,M.R., Maniatis,T., Zinn,K. and Green,M.R. (1984) *Nucleic Acids. Res.*, **12**, 7035–7056.
Mount,S.M., Petterson,I., Hinterberger,M., Karmas,A. and Steitz,J.A. (1983) *Cell*, **33**, 509–518.
Padgett,R.A., Mount,S.M., Steitz,J.A. and Sharp,P.A. (1983) *Cell*, **35**, 101–107.
Padgett,R.A., Grabowski,P.J., Konarska,M.M. and Sharp,P.A. (1986) *Annu. Rev. Biochem.*, **55**, 1119–1150.
Perkins,K.K., Furneaux,H.M. and Hurwitz,J. (1986) *Proc. Natl. Acad. Sci. USA*, **83**, 887–891.
Pikielny,C.W. and Rosbash,M. (1986) *Cell*, **45**, 869–877.
Pikielny,C.W., Rymond,B.C. and Rosbash,M. (1986) *Nature*, **324**, 341–345.
Reeves,W.H., Fisher,D.E., Wisniewolski,R., Gottlieb,A.B. and Chiorazzi,N. (1986) *N. Engl. J. Med.*, **315**, 105–111.
Ruskin,B., Krainer,A.R., Maniatis,T. and Green,M.R. (1984) *Cell*, **38**, 317–331.
Ruskin,B. and Green,M.R. (1985a) *Cell*, **43**, 131–142.
Ruskin,B. and Green,M.R. (1985b) *Nature*, **317**, 732–734.
Rymond,B.C. and Rosbash,M. (1986) *EMBO J.*, **5**, 3517–3523.
Sharp,P.A. (1987) *Science*, **235**, 766–771.
Zhuang,Y. and Weiner,A.M. (1986) *Cell*, **46**, 827–835.

*Received on April 23, 1987; revised on May 7, 1987*